


IFN- γ stimulated murine and human neurons mount anti-parasitic defenses against the intracellular parasite *Toxoplasma gondii*

Received: 24 November 2021

Accepted: 19 July 2022

Published online: 08 August 2022

 Check for updatesSambamurthy Chandrasekaran¹, Joshua A. Kochanowsky^{2,6}, Emily F. Merritt², Joseph S. Lagas³, Ayesha Swannigan⁴ & Anita A. Koshy^{1,2,5} 

Dogma holds that *Toxoplasma gondii* persists in neurons because neurons cannot clear intracellular parasites, even with IFN- γ stimulation. As several recent studies questioned this idea, here we use primary murine neuronal cultures from wild type and transgenic mice in combination with IFN- γ stimulation and parental and transgenic parasites to reassess IFN- γ dependent neuronal clearance of intracellular parasites. We find that neurons respond to IFN- γ and that a subset of neurons clear intracellular parasites via immunity regulated GTPases. Whole neuron reconstructions from mice infected with parasites that trigger neuron GFP expression only after full invasion reveal that ~50% of these *T. gondii*-invaded neurons no longer harbor parasites. Finally, IFN- γ stimulated human pluripotent stem cell derived neurons show an ~50% decrease in parasite infection rate when compared to unstimulated cultures. This work highlights the capability of human and murine neurons to mount cytokine-dependent anti-*T. gondii* defense mechanisms in vitro and in vivo.


A select number of highly divergent intracellular microbes (e.g. measles virus, polio virus, *Toxoplasma gondii*) cause infections of the central nervous system (CNS). Though these microbes infect many cell types, in the CNS, neurons are often preferentially infected. One commonly cited reason for this neuron predominance is that neurons lack the ability to mount traditional cell-intrinsic immune responses^{1–3}. For example, neurons have low baseline levels of MHC I and STAT1^{1,4–6}. However, considerable evidence shows that neurons can respond to type I and type II interferons^{4,5,7,8} and clear certain viral pathogens (e.g. Sindbis virus^{9,10} and vesicular stomatitis virus¹¹). Limited work has been done on the capabilities of neurons to clear non-viral pathogens.

Toxoplasma gondii is a protozoan parasite that naturally infects most warm-blooded animals, including humans and mice. In most immune competent hosts, *T. gondii* establishes a persistent or latent infection by switching from its fast growing lytic form (the tachyzoite) to its slow growing, encysting form (the bradyzoite). In humans and mice, the CNS is a major organ of persistence and neurons are the

principal cell in which *T. gondii* cysts are found^{12–15}. IFN- γ is essential for control of *T. gondii* both systemically and in the CNS^{16,17}, in part through the activation of the immunity regulated GTPase system (IRGs) which is critical for parasite control in hematopoietic and non-hematopoietic cells^{18–20}. Based upon these findings and in vitro studies showing that *T. gondii* readily invades murine astrocytes and neurons, but only IFN- γ -stimulated astrocytes—not IFN- γ -stimulated neurons—clear intracellular parasites^{19,21–23}, the model of CNS toxoplasmosis was that during natural infection parasites enter the CNS, invade both astrocytes and neurons, after which astrocytes kill the intracellular parasites, leaving the immunologically incompetent neuron as the host cell for the persistent, encysted form of the parasite.

Several recent findings have called this model into question. Pan-cellular ectopic expression of an MHC I allele (H-2 L^d) associated with low levels of CNS persistence^{24,25} leads to a lower CNS parasite burden than when mice lack expression of this MHC I allele in neurons only²⁶. Moreover, the use of a Cre-based system that permanently marks CNS

¹BIO5 Institute, University of Arizona, Tucson, AZ, USA. ²Department of Immunobiology, University of Arizona, Tucson, AZ, USA. ³Undergraduate Biology Research Program, University of Arizona, Tucson, AZ, USA. ⁴Undergraduate Research Opportunities Consortium, University of Arizona, Tucson, AZ, USA. ⁵Department of Neurology, University of Arizona, Tucson, AZ, USA. ⁶Present address: University of California, Los Angeles, CA, USA.

 e-mail: akoshy@arizona.edu

cells that have been injected with *T. gondii* proteins^{27,28}, revealed that parasites extensively interact with neurons and that the majority (>90%) of these *T. gondii*-injected neurons do not actively harbor cysts^{15,27}. Together these in vivo studies question the prior model by raising the possibility that neurons clear intracellular parasites.

In this work, we use primary murine neuronal cultures from wild type and genetically modified mice in combination with cytokine stimulation and parental and transgenic parasites, including a new engineered *T. gondii*-Cre line, to reassess the ability of neurons to clear intracellular parasites in the setting of IFN- γ stimulation. Given the prior conflicting in vitro and in vivo findings, our data reveal that neurons respond to IFN- γ , including up-regulating the IRGs, and that a subset of neurons (~20%) clear intracellular parasites via the IRGs. In addition, in Cre reporter mice infected with *T. gondii*-Cre parasites that mark CNS cells only after full invasion, whole neuron reconstructions show that ~50% of these *T. gondii*-invaded neurons no longer harbor parasites. Finally, IFN- γ stimulation of human pluripotent stem cell derived neurons (hPSC-neurons) leads to an ~50% decrease in parasite infection rate when compared to unstimulated, infected cultures. Collectively, these data highly suggest that IFN- γ stimulation leads to parasite resistance in murine and human neurons and that a subset of murine neurons clear intracellular parasites both in vitro and in vivo, likely via the IRGs.

Results

IFN- γ stimulated primary pure murine cortical neurons show classical IFN- γ responses

As *T. gondii* primarily infects and encysts in the cortex^{29–31}, we sought to determine the response of cortical neurons to IFN- γ stimulation. To accomplish this goal, we exposed pure primary murine cortical neuronal cultures to 100 U/ml of IFN- γ or vehicle control for 4 and 24 h, followed by harvesting of total RNA. We chose these time points because prior work showed that hippocampal neurons have a delayed IFN- γ response⁵. After harvesting the RNA, we used quantitative real time-PCR (qRT-PCR) to quantify transcript levels of traditional IFN- γ -response genes (*STAT1*, *IRF1*, *MHC-I*) as well as the effector components of the IRG system (*Irga6*, *Irgb6*, and *Gbp2*)^{32,33}. We found that *STAT1*, the classical transcription factor that drives the expression of many IFN- γ response genes, and *IRF1* were highly upregulated (4 h: 3–5 log₂ fold; 24 h: 5–7 log₂ fold) compared to unstimulated neurons (Fig. 1A), while *MHC-I* showed a more modest level of upregulation (~2 log₂ fold) and only at 24 h. In addition, consistent with findings in non-neuronal murine cells, compared to unstimulated neurons, IFN- γ stimulated neurons also significantly up-regulated *Irga6*, *Irgb6*, and *Gbp2* (4 h: 4–7 log₂ folds; 24 h: 7–9 log₂ folds) (Fig. 1A)^{34–36}. To determine how these increased transcript levels translated to protein levels, we isolated total protein lysates from unstimulated and IFN- γ stimulated cultures. For *STAT1*, we blotted both for total *STAT1* and for phosphorylated *STAT1* (p*STAT1*), the active form that enters the nucleus and binds DNA. Compared to unstimulated cultures, IFN- γ stimulated cultures showed a >10-fold increase in protein levels for total *STAT1* and p*STAT1* at 24 h post-stimulation and a >35-fold increase at 48 h post-stimulation (Fig. 1B, C). The undetectable level of total *STAT1* in unstimulated neurons is consistent with previously published data suggesting that neurons have low or no constitutive amounts of *STAT1*³⁷. Similarly, at 24 h post-stimulation, the IRG complex effector proteins *Irga6* and *Irgb6* increased an ~7-fold and 10-fold respectively over unstimulated cultures, a level that was maintained at 48 h post stimulation (Fig. 1B, C).

To confirm that the detected changes were primarily driven by neurons and not by glial cells that commonly cause low levels of contamination in “pure” neuronal cultures, we stained the cultures to determine what percentage of cells were neurons, astrocytes, or microglia. These analyses showed that our cultures were consistently 95% neurons and 5% astrocytes; no microglia were observed

(Supplementary Fig. 1). To determine the level of nuclear translocation of p*STAT1* at the single neuron level, we stained unstimulated and stimulated (100 U/ml for 24 h) primary neuron cultures with DAPI and antibodies against *Tuj1*, a neuronal marker, and p*STAT1*. We then quantified the p*STAT1* signal intensity in *Tuj1*⁺ nuclei. In unstimulated cultures, we observed very little p*STAT1* signal in *Tuj1*⁺ nuclei (MFI 2236 ± 353.24, mean ± SEM) (Fig. 1D). Conversely, IFN- γ stimulated neurons showed an ~10–90-fold increase in p*STAT1* staining in *Tuj1*⁺ nuclei (Fig. 1D).

Together these data show that IFN- γ stimulated primary murine cortical neuron cultures upregulate IFN- γ response genes and proteins in a delayed manner consistent with what has been observed in hippocampal neurons⁵. The upregulated genes and proteins include *STAT1* and the IRG genes known to be required for IFN- γ -dependent killing of intracellular parasites in murine non-neuronal cells³³. Collectively, these data suggest that IFN- γ stimulated murine cortical neurons upregulate the appropriate machinery to clear intracellular parasites via the IRG system.

IFN- γ pre-stimulation leads to a decrease in the percentage of *T. gondii*-infected neurons

To address neuronal capability for clearing intracellular parasites, we infected IFN- γ stimulated or unstimulated neurons with representative strains from the three genetically distinct canonical *T. gondii* strain types (type I (RH), II (Prugniaud), and III (CEP)), which differ in acute virulence in mice^{38,39}. We quantified neuron infection rates at 3, 12, and 24 h post infection (hpi). At 3 hpi, stimulated and unstimulated cultures showed a similar infection rate, regardless of infecting strain (Fig. 2A–C). At 12 and 24 hpi, the type I strain continued to show the same infection rate in both vehicle and IFN- γ stimulated cultures (Fig. 2A). Conversely, IFN- γ stimulated cultures infected with type II or type III parasites showed an ~25% decrease in infection rate at 12 and 24 hpi, (Fig. 2A–C).

GCre-expressing parasites show that neurons clear parasites in response to IFN- γ

While the prior data suggested that IFN- γ stimulated neurons might clear intracellular parasites in a strain-specific manner, these findings could also be explained by decreased rates of late invasion by type II and type III parasites in IFN- γ stimulated neurons. A late invasion defect is possible because clearance assays in neurons are limited by the inability to synchronize infection or vigorously wash off uninvaded parasites as either procedure causes widespread neuronal death. To distinguish between a late invasion defect and true clearance of intracellular parasites, we needed a way to specifically track neurons that were infected and subsequently cleared the intracellular parasite. As noted above, we had previously developed a Cre-based system that leads to GFP expression only in host cells injected with *T. gondii* proteins. In this system, Cre is fused to toxoflin, a rhoptry protein (ROP). ROPs are parasite proteins that are injected into host cells *prior to invasion*, which means that parasite-triggered host cell expression of GFP does not require parasite invasion (i.e., aborted invasion) (Fig. 2D). Thus, RCre (ROP::Cre)-expressing parasites do not help us distinguish between increased aborted invasion versus clearance of intracellular parasites. One way to address this issue would be to fuse Cre to GRA16, a dense granule protein (GRA) that is released into host cells only *after invasion*^{40–43}. Thus, GCre (GRA::Cre)-expressing parasites should not cause Cre-mediated recombination in the setting of aborted invasion and should only identify host cells that were or had previously been infected (Fig. 2D).

To test this potential solution, we engineered type II parasites to express an HA-tagged GCre (II-GCre). Using immunofluorescent assays and plaque assays, we determined that GCre was expressed, did not localize to the rhoptries, and that the expression of GCre did not affect overall parasite viability (Supplementary Fig. 2). To test the capability

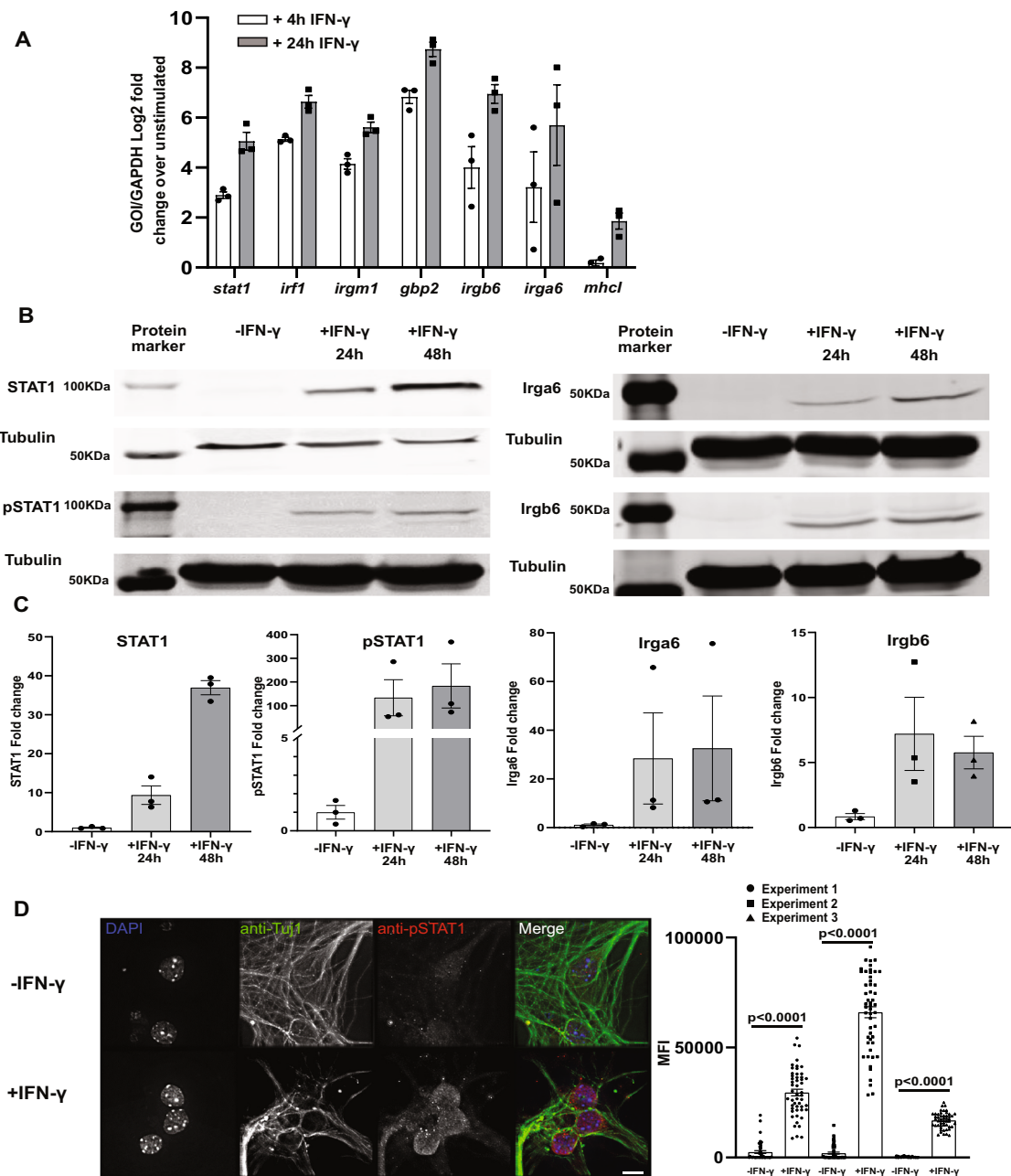


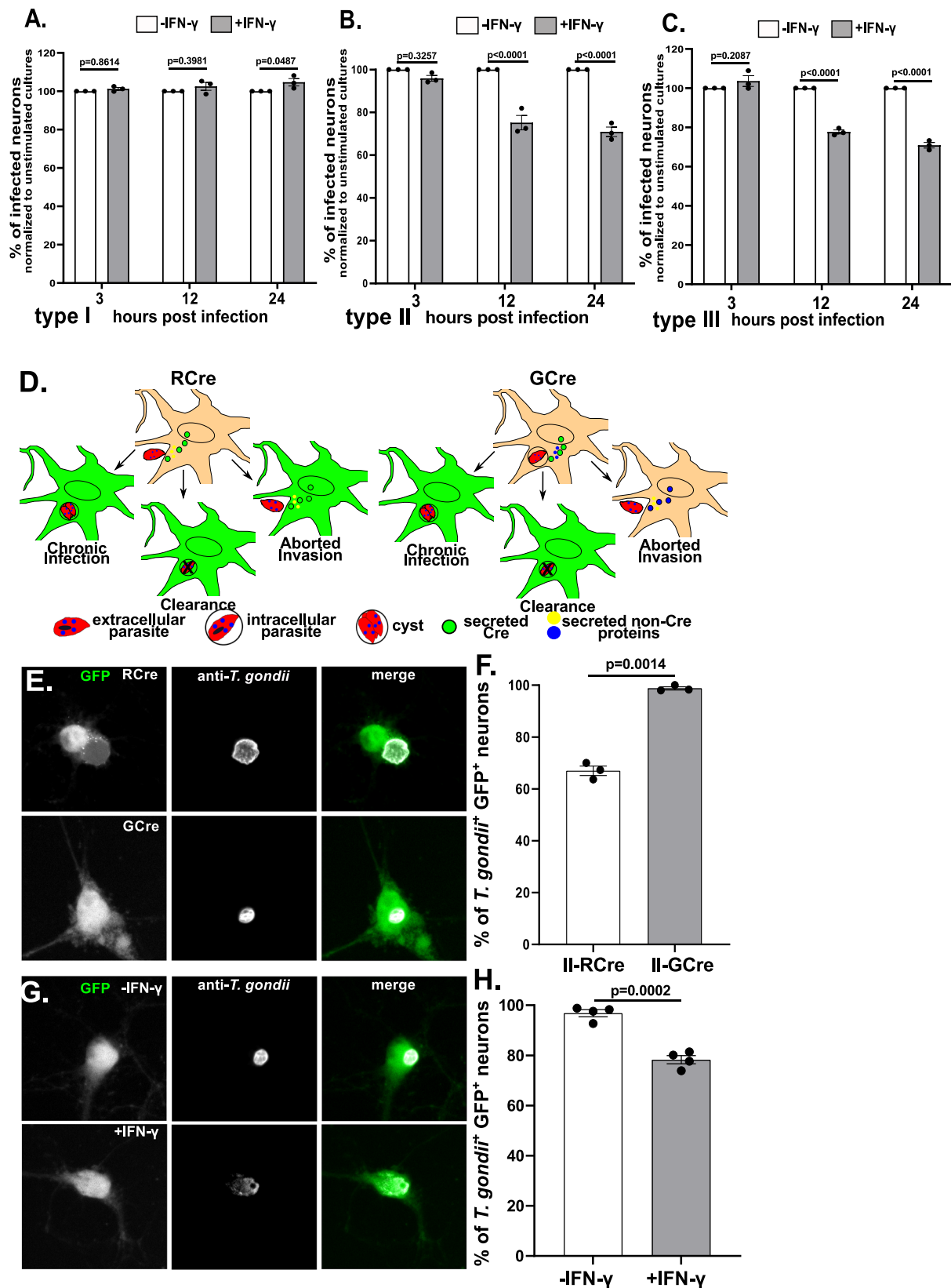
Fig. 1 | IFN- γ stimulated primary murine neurons show intact IFN- γ signaling pathway and express genes involved in *T. gondii* clearance. Primary neurons cultures were stimulated with vehicle or IFN- γ (100 U/ml), followed by RNA or protein extraction or immunofluorescent assays. **A** Quantification of specified genes using qRT-PCR. **B** Representative images of western blots for specified proteins from unstimulated and IFN- γ stimulated cultures. **C** Densitometric quantification of western blots. Proteins of interest are normalized to β -tubulin and then shown as a fold change over unstimulated cultures. For **A**, **C** Bars, mean \pm SEM. $N = 3$

independent experiments. **D** Images: Representative images of unstimulated or IFN- γ stimulated neurons stained as indicated. Merge image: blue = DAPI, green = anti-Tuj1 (anti-neuron antibody) = green, red = anti-pSTAT. Scale bar = 5 μ m. Graph: Quantification of the mean fluorescent intensity (MFI) of pSTAT1 nuclear signal in unstimulated or IFN- γ stimulated Tuj1⁺ cells. $N = 48$ –51 nuclei/experiment, 3 independent experiments. Bars, mean \pm SD. Unpaired t-test with Welch's correction. **A–C**, **D** graph Source data are provided as a Source Data file.

of II-GCre parasites to trigger Cre-mediated recombination, we infected Cre reporter fibroblasts that express GFP only after Cre-mediated recombination²⁸ with II-RCre parasites, II-GCre parasites, or parental type II parasites (no Cre expression). At 24 hpi, we observed that both II-RCre parasites and II-GCre parasites caused host cell expression of GFP, while the parental strain did not (Supplementary Fig. 3A, B). Compared to II-RCre parasites, II-GCre parasites were less efficient at triggering Cre-mediated recombination (>90 vs. 50%, Supplementary

Fig. 3B), which was expected because host cell-exported GRA proteins show decreased exportation when fused to ordered proteins^{41,44,45}.

Having confirmed that II-GCre parasites trigger Cre-mediated recombination, we next assessed the capability of II-GCre parasites to identify only infected cells. To test this possibility, we infected cortical neuron cultures from Cre reporter mice for 72 h, which was the time point when we saw robust neuronal GFP expression. In II-RCre infected cultures, 67 \pm 1.82% of GFP⁺ neurons were infected. In II-GCre infected



cultures, $98 \pm 0.62\%$ of GFP⁺ neurons were infected (Fig. 2E, F). As cultured neurons do not divide, we assume the ~30% of uninfected GFP⁺ neurons in II-RCre infected cultures arise from aborted invasion (Fig. 2F). More importantly, that ~100% of GFP⁺ neurons are infected when using II-GCre parasites confirms that II-GCre parasites trigger Cre-mediated recombination only after fully invading the host cell.

Having engineered parasites that only identify fully infected neurons, we next tested how IFN- γ pre-stimulation affected the rate of infection of GFP⁺ neurons by stimulating Cre reporter neuron cultures with vehicle or IFN- γ (100 U/ml) for 24 h prior to infection with II-GCre parasites. Consistent with previous results (Fig. 2F), in the vehicle treated cultures, $97 \pm 1.4\%$ of GFP⁺ neurons harbored a parasite

Fig. 2 | IFN- γ stimulated neurons clear intracellular parasites. Primary neuron cultures were treated as in Fig. 1. **A** Graph of the percentage of infected neurons, normalized to the unstimulated culture, for type I parasites. **B** As in **A** except for type II parasites. **C** As in **A** except for type III parasites. **A–C** Bars mean \pm SEM. $N = 759$ – 1538 neurons/*T. gondii* strain/experiment, 3 independent experiments. 2-way ANOVA with Sidak's multiple comparisons. **D** Schematic of host cells labeled by RCre versus GCre parasites. *Left*, With RCre parasites the Cre fusion protein is secreted prior to invasion, leading to GFP-expressing neurons that arise from: (i) injection, invasion, and chronic infection, (ii) injection and invasion followed by neuronal clearance of the parasite, and (iii) injection of the protein *without* invasion (aborted invasion). *Right*, with GCre parasites the Cre fusion protein is secreted post invasion, leading to GFP-expressing neurons that arise from: (i) invasion and

persistent infection or (ii) invasion followed by clearance of the parasite, but not from aborted invasion. **E** Representative images of GFP⁺ neurons infected with listed parasites. *Merge image*: green = GFP, white = parasites stained with anti-*T. gondii* antibodies. Scale bar = $10\ \mu\text{m}$. **F** Graph of the percentage of infected GFP⁺ neurons at 72 hpi (unstimulated cultures). $N = 300$ neurons/experiment, 3 independent experiments. **G** Representative images of unstimulated or IFN- γ stimulated primary neurons infected with II-GCre parasites at 72 h. *Merge image*, as in **E**. Scale bar = $10\ \mu\text{m}$. **H** Graph of the percentage of infected GFP⁺ neurons at 72 hpi. $N = 290$ – 452 neurons/experiment, 4 independent experiments. **F, H** Bars mean \pm SEM. Unpaired t-test with Welch's correction. **A–C, F, H** Source data are provided as a Source Data file.

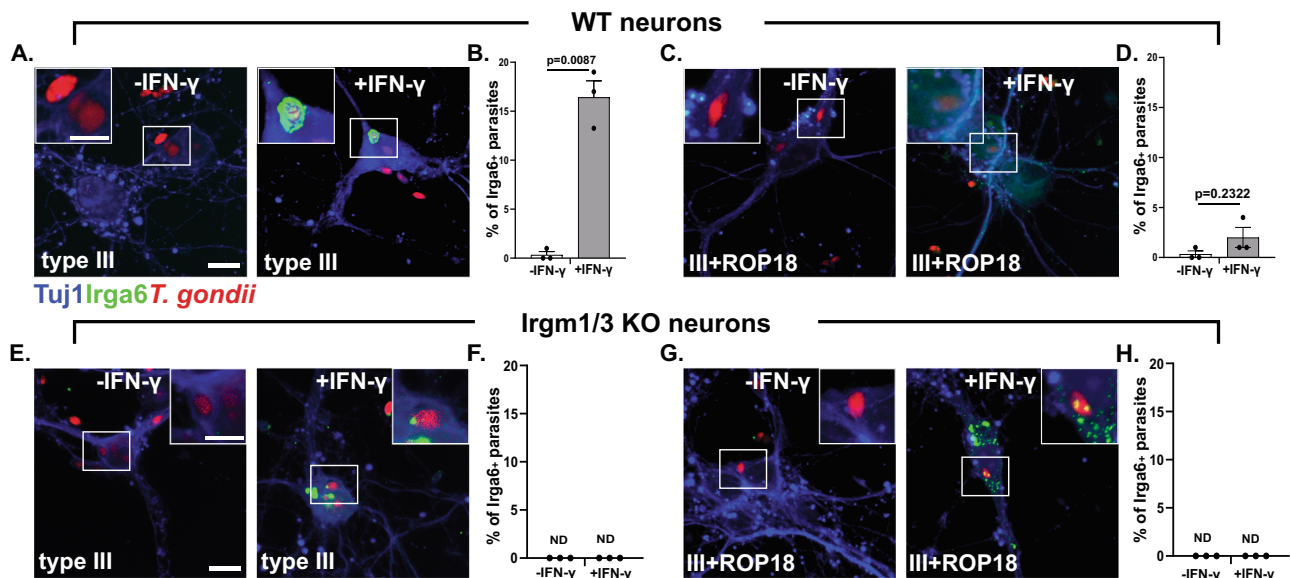


Fig. 3 | IFN- γ stimulated wild type murine show increased loading of Irga6 onto the PVM of type III parasites. Primary neuron cultures were treated as in Fig. 1, followed by infection with listed *T. gondii* strains. At 12 hpi cultures were fixed and stained with anti-Irga6 and anti-Tuji1 antibodies. The stained cultures were analyzed by confocal microscope. **A** Representative images of stained cultures from wild type (WT) mice infected with type III parasites. Blue = anti-Tuji1 antibodies, green = anti-Irga6 antibodies, red = mCherry expressing parasites. **B** Quantification of the percentage of Irga6⁺ parasitophorous vacuoles (PVs) in the setting of vehicle

or IFN- γ pre-stimulation. **C** Representative images as in **A** except infected with III + ROP18 parasites. **D** As in **B**. **E** Representative images as in **A** except using cultures from *Irgm1/3* KO mice. **A, E** Scale bar = $10\ \mu\text{m}$ full image, $5\ \mu\text{m}$ inset. **F** As in **B**. **G** Representative images as in **C** except using *Irgm1/3* KO neurons. **H** As in **B**. **B, D, F, H** Bars - mean \pm SEM, $N = 100$ – 200 PVs/experiment, 3 independent experiments. ND = not detected. Unpaired t-test with Welch's correction. Source data are provided as a Source Data file.

(Fig. 2G, H). Conversely, in the setting of pre-treatment with IFN- γ , now only $78 \pm 1.6\%$ GFP⁺ neurons harbored parasites. These data suggest that the decrease in the rate of infection with type II and type III parasites in IFN- γ stimulated neurons (2B, C) is primarily mediated by IFN- γ stimulated neurons clearing intracellular parasites, rather than IFN- γ stimulation leading to decreased parasite invasion.

In IFN- γ stimulated murine neurons Irga6 loads onto the PVM in a *Irgm1/3*-dependent manner

As IFN- γ stimulated neurons up-regulate the IRG effectors (Fig. 1) and a portion clear IRG-sensitive intracellular parasites (Fig. 2), we next sought to determine if neurons use the IRG system to mediate IFN- γ -dependent killing of *T. gondii*. As loading of IRGs onto *T. gondii*'s parasitophorous vacuolar membrane (PVM) is indispensable for parasite clearance in IFN- γ stimulated non-neuronal cells⁴⁶ and as Irga6 is one of the effectors that loads onto the PVM³³, we analyzed the percentage of parasitophorous vacuoles (PVs) that were also Irga6⁺ in unstimulated and IFN- γ stimulated neurons infected with type III parasites. Consistent with findings in non-neuronal murine cells, we found that in unstimulated neurons, type III parasite PVs showed almost no Irga6 loading, while PVs in IFN- γ stimulated neurons showed an 8-fold increase in Irga6 loading (Fig. 3A, B). To further confirm these

findings, we also used a type III "IRG-resistant" strain¹⁵. This strain is engineered to express high levels of ROP18 (III + ROP18). ROP18 is a *T. gondii* kinase that phosphorylates Irga6 thereby preventing PV loading and effector oligomerization⁴⁷. The parental type III strain has minimal expression of ROP18 because of an insertion in the promoter region of the *rop18* gene; it is this lack of ROP18 expression that renders the parental strain susceptible to the IRGs^{48,49}. In cultures infected with III + ROP18 parasites, as expected, we now found almost no Irga6⁺ PVs even in the setting of IFN- γ stimulation (Fig. 3C, D). Finally, to confirm that IRG-loading followed the same principles in neurons as in non-neuronal cells, we used neurons from mice that lack the regulatory IRG components (*irgm1* and *irgm3*)⁵⁰, which for simplicity we will call *Irgm1/3* KO mice. These regulatory components tether the effector components (e.g. Irga6) to the appropriate organelle until triggered to release the effectors onto the PV⁵¹; in cells that lack these proteins, the effectors inappropriately load onto host cell organelles and no longer target the PV⁵². As expected, in *Irgm1/3* KO neurons, we found an increase in Irga6 aggregates in the setting of IFN- γ stimulation but no specific loading onto PVs regardless of IFN- γ stimulation or infecting strain (Fig. 3E–H).

Together, these data demonstrate that neuronal Irga6 loads onto the PVM of intracellular IRG-sensitive parasites in the setting of IFN- γ

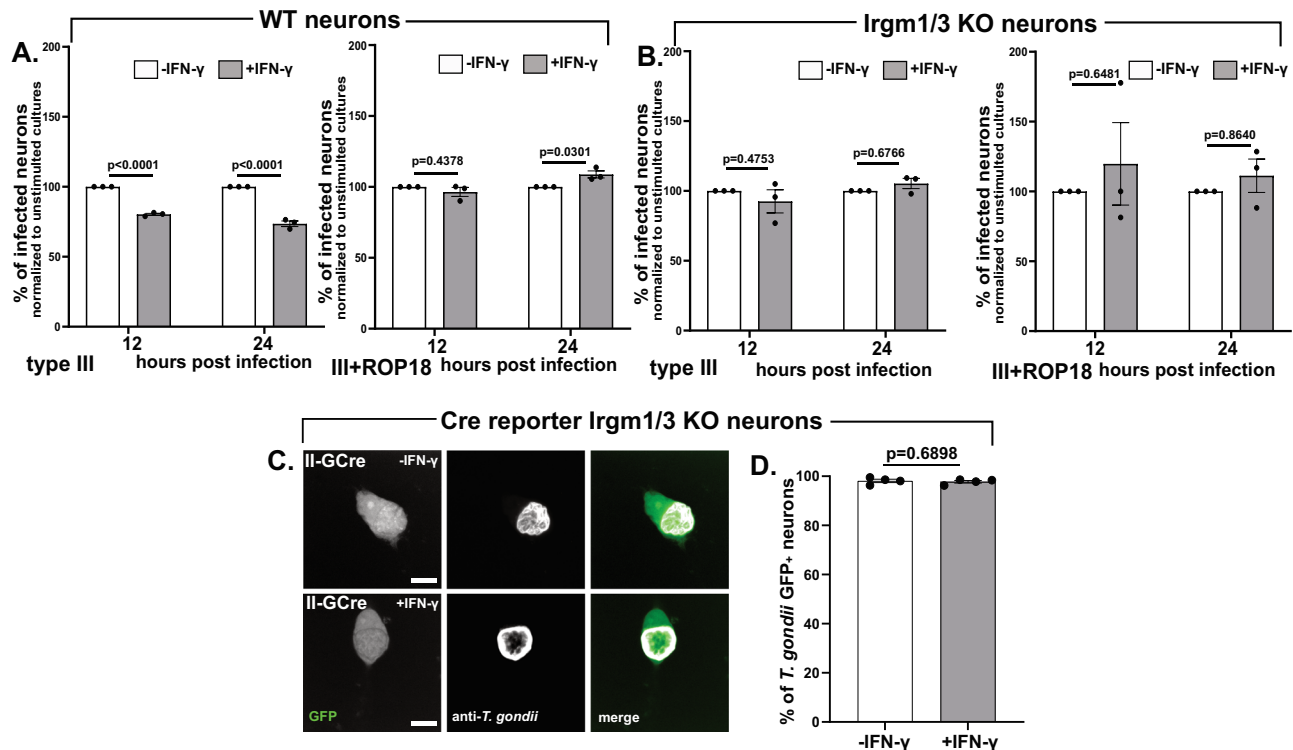


Fig. 4 | An intact IRG system is required for IFN- γ -dependent murine neurons clearance of intracellular parasites. Primary neuron cultures from WT (Cre reporter), *Irgm1/3* KO, or Cre reporter *Irgm1/3* KO mice were treated as in Fig. 1 followed by infection with listed *T. gondii* strains. **A** Graph of the percentage of infected WT neurons at listed time points for type III parasites (left graph) and III + ROP18 parasites (right graph), normalized to the unstimulated culture. **B** As in **A** except using *Irgm1/3* KO neurons and either type III parasites (left graph) or III + ROP18 parasites (right graph). **A, B** At the listed time points, cultures were fixed, stained, and analyzed as in Fig. 2A. Bars mean \pm SEM., $N = 731$ –1448 neurons/ $T.$

gondii strain/experiment, 3 independent experiments. 2-way ANOVA with Sidak's multiple comparisons. **C** Representative images of GFP⁺ neurons from Cre reporter *Irgm1/3* KO mice infected with II-GCre parasites. Merge image: Green = GFP, white = parasites stained with anti-*T. gondii* antibodies. Scale bars = 10 μ m. **D** Graph of the percentage of infected GFP⁺ neurons. Bars, mean \pm SEM. $N = 389$ –506 neurons analyzed/experiment, 4 independent experiments. Unpaired t-test with Welch's correction. **C, D** Cultures were infected, fixed, stained, and analyzed as in Fig. 2F. **G, A, B, D** Source data are provided as a Source Data file.

pre-stimulation and when neurons have an intact IRG-system. These data strongly suggest that murine neurons use the IRG system for IFN- γ -dependent clearance/killing of intracellular parasites.

IFN- γ stimulated murine neurons kill intracellular parasites using the IRG system

While the preceding data strongly suggests that murine neurons deploy the IRG-system to kill intracellular parasites in the setting of IFN- γ stimulation, they do not show that the IRG-system is essential for neuronal killing. To directly test this possibility, we took several approaches. First, we tested the ability of IFN- γ stimulated, wild type neurons to clear III + ROP18 parasites which show no *Irga6*⁺ loading even in the setting of IFN- γ stimulation (Fig. 3C, D). Indeed, in murine neuronal cultures infected with III + ROP18 parasites, we found the same rate of infection over time, regardless of IFN- γ stimulation (Fig. 4A). Second, we infected *Irgm1/3* KO neuronal cultures with parental (type III, IRG-sensitive) or III + ROP18 parasites (IRG-resistant) and with or without IFN- γ pre-stimulation. We again found the same rate of infection, regardless of what strain we utilized (IRG-sensitive or resistant) and IFN- γ pre-stimulation state (Fig. 4B). As a final method of confirming that the lack of IRGs specifically affected intracellular parasites, we bred *Irgm1/3* KO mice to Cre reporter mice to yield mice homozygous for the Cre reporter construct and that lack both *Irgm1* and *Irgm3*. We then generated neuronal cultures, which we stimulated with vehicle or IFN- γ , followed by infection with II-GCre parasites. In these cultures, -98% (-IFN- γ : 98.12 \pm 0.67%; +IFN- γ : 97.8% \pm 0.53) of GFP⁺ neurons were infected, regardless of IFN- γ stimulation status (Fig. 4C, D).

Collectively, these data definitively show that in vitro IFN- γ stimulated neurons to kill intracellular IRG-sensitive parasites via the IRG system.

Neurons clear intracellular parasites in vivo

Having shown that IFN- γ stimulated neurons clear intracellular parasites in vitro, we sought to determine if neurons cleared parasites in vivo. As II-GCre parasites trigger Cre-mediated recombination only after full host cell invasion (Fig. 2C), we reasoned that if we found GFP⁺, parasite⁻ neurons in Cre reporter mice infected with II-GCre parasites, these neurons must have cleared the invading parasite. To assess for GFP⁺ parasite⁻ neurons in vivo, we created whole neuron reconstructions from Hoechst-stained brain sections from 21 day post-infection (dpi) II-GCre infected mice^{53,54} (Fig. 5A, B). Within these GFP⁺ neurons, we looked for areas that lacked GFP (Fig. 5B) because the PV excludes host cell GFP. We then confirmed that these areas contained parasites using Hoechst staining of parasite DNA (Fig. 5C, Supplementary Fig. 4). To confirm that our method for identifying parasites was accurate, for a subset of brain sections, we also stained the sections with either of two different anti-*T. gondii* antibodies. As expected, when we identified areas lacking GFP and showing Hoechst-stained parasite DNA, these areas were also positive for anti-*T. gondii* antibody staining (Fig. 5D, Supplementary Fig. 4A, B). Out of 35 reconstructed GFP⁺ neurons, we found that 17 (~50%) showed no evidence of persistent parasite infection (Fig. 5E). These data highly suggest that, in vivo, a substantial percentage of infected murine neurons clear intracellular parasites.

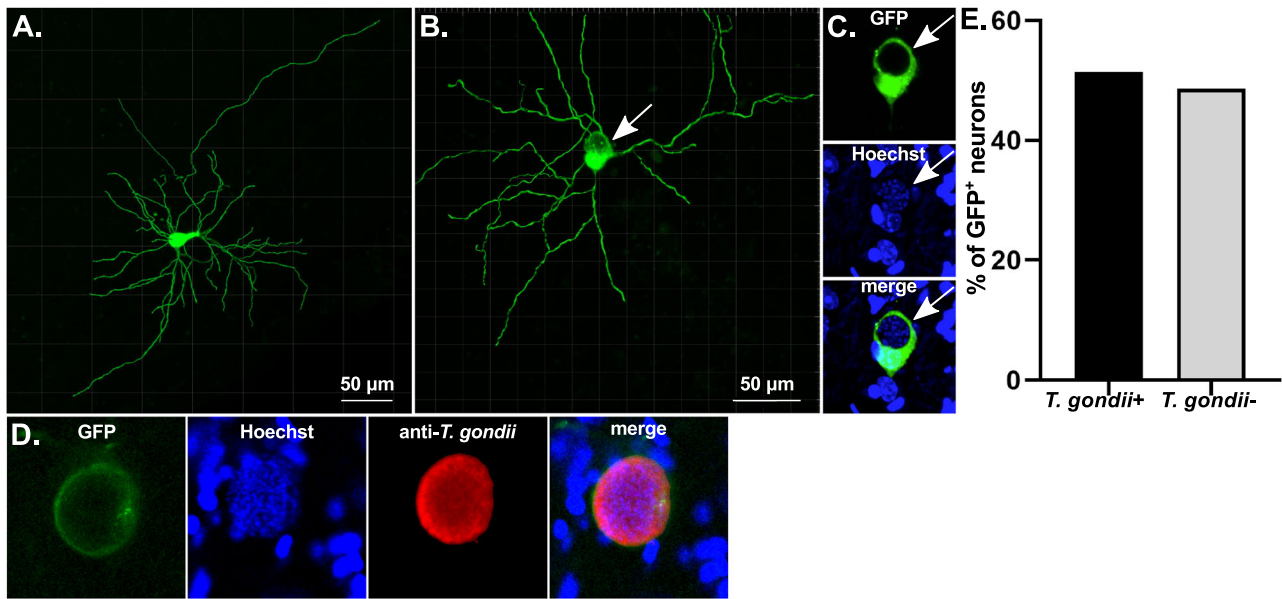


Fig. 5 | Fifty percent of GFP⁺ neurons in mice infected with GCre parasites do not harbor parasites. Cre reporter mice were infected with II-GCre parasites. At 21 dpi, brains were harvested and sagittally sectioned into 200 μ m thick sections. Sections were cleared, stained with Hoechst \pm anti-*T. gondii* antibodies, and imaged at 40 \times on a confocal microscope. Neurons in resulting images were rendered using Imaris software. **A** Representative rendering of a GFP⁺ neuron in which no parasites were identified. **B** As in **A** except now with a GFP⁺ neuron in which parasites were identified. White arrow shows parasites within neuron soma. **C** Single plane of soma from **B** top image: green = GFP, middle image: blue = Hoechst, bottom image: merge. **D** Representative image of a single plane of a rendering from a section stained with anti-*T. gondii* antibodies. Note that the parasite nuclei identified by Hoechst staining co-localize with the anti-*T. gondii* antibody staining. Green = GFP, blue = Hoechst, red = anti-*T. gondii* antibodies. **E** Graph of the percentage of rendered GFP⁺ neurons containing parasites (*T. gondii*⁺/infected) or not containing parasites (*T. gondii*⁻/uninfected). *N* = 35 neurons from 5 mice. Source data are provided as a Source Data file.

Note the GFP displacement, suggesting parasite presence within the neuron, which is then confirmed by visualization of parasite nuclei stained with Hoechst (blue). **D** Representative image of a single plane of a rendering from a section stained with anti-*T. gondii* antibodies. Note that the parasite nuclei identified by Hoechst staining co-localize with the anti-*T. gondii* antibody staining. Green = GFP, blue = Hoechst, red = anti-*T. gondii* antibodies. **E** Graph of the percentage of rendered GFP⁺ neurons containing parasites (*T. gondii*⁺/infected) or not containing parasites (*T. gondii*⁻/uninfected). *N* = 35 neurons from 5 mice. Source data are provided as a Source Data file.

IFN- γ stimulated human neurons show resistance to *T. gondii* infection

Having shown that murine neurons clear a portion of intracellular parasites in vitro and in vivo, we sought to translate these findings to human neurons. While mice and murine cells are good models for human infection (both are naturally infected with *T. gondii*, have the CNS as a major organ of persistence, have neurons as the major host cell for cysts, and require IFN- γ and CD8 T cells to control toxoplasmosis), differences exist between the two. In the current context, the most relevant difference is that human cells lack the expansive range of IRGs that mice have and instead rely on alternative mechanisms, which can vary by cell type, for IFN- γ -dependent control of *T. gondii*⁵⁵. A prior study has shown that when IFN- γ stimulated human stem cell (hSC)-derived neurons are co-cultured with infected monocytes, parasite luciferase expression decreases compared to co-cultures of infected monocytes and unstimulated hSC-derived neurons⁵⁶. As this work did not determine what caused the decrease in parasite luciferase expression, it is impossible to determine if the IFN- γ responses were being driven by effects on the neurons, infected monocytes, or both. Thus, we sought to more directly determine how IFN- γ stimulation influenced control of *T. gondii* in human neurons. To accomplish this goal, we derived neurons from human neuroprogenitor cells reprogrammed from an embryonic pluripotent stem cell line. After confirming that the hPSC neurons expressed appropriate cortical neuronal markers (Supplementary Fig. 5), we pre-treated hPSC neurons with human IFN- γ for 24 h, followed by infection with type II or III parasites. We then quantified the neuron infection rate at 3, 12, and 24 hpi via epifluorescent microscopy (Fig. 6). At 3 hpi, regardless of infecting strain, we found equivalent neuron infection rates between unstimulated and IFN- γ stimulated cultures. At 12 and 24 hpi, IFN- γ stimulated cultures showed a $\geq 50\%$ decrease in the neuron infection rate compared to unstimulated cultures (Fig. 6). These data highly

suggest that human neurons also mount anti-parasitic defenses in response to IFN- γ stimulation.

Discussion

In this study, we sought to address the question: can neurons clear intracellular parasites? Using in vitro primary murine neurons from wild type and transgenic mice in combination with IFN- γ pre-stimulation and transgenic parasites, this work shows that a portion of murine neurons can and do clear intracellular parasites in an IFN- γ -dependent, IRG-dependent manner. Using our new II-GCre parasites, which trigger host cell mediated recombination only after full invasion, we also show that $\sim 50\%$ of neurons clear parasites in vivo. Finally, using hPSC neurons, we translated our findings to human neurons, showing that IFN- γ pre-stimulation decreases the infection rate by $\sim 50\%$.

The data presented are the first to show that IFN- γ pre-stimulation enables human and murine neurons to partially resist successful infection by an intracellular eukaryotic pathogen. Importantly, in murine neurons, we leveraged *T. gondii* biology to show that this resistance was secondary to clearance of intracellular parasites (Fig. 2H), not simply an invasion defect (an important distinction in cultures where procedures such as aggressively washing off extracellular parasites cannot be done). In addition, our finding that IFN- γ stimulated murine neurons clear parasites in an IRG-dependent manner explains why a prior study found that IFN- γ stimulated primary murine neurons failed to clear intracellular parasites. The prior study, which was done at a time when neither the IRGs nor the parasite mechanisms to block the IRGs had been fully described, used a type I strain (RH) that we now know is IRG-resistant^{23,47}. Consistent with the possibility that the use of this strain led to the negative findings, we also found no evidence for IFN- γ -dependent neuronal clearance when we infected with this IRG-resistant strain (Fig. 2A). In addition to addressing this prior work, our findings also potentially offer a mechanism for the recent work showing that MHC class I expression

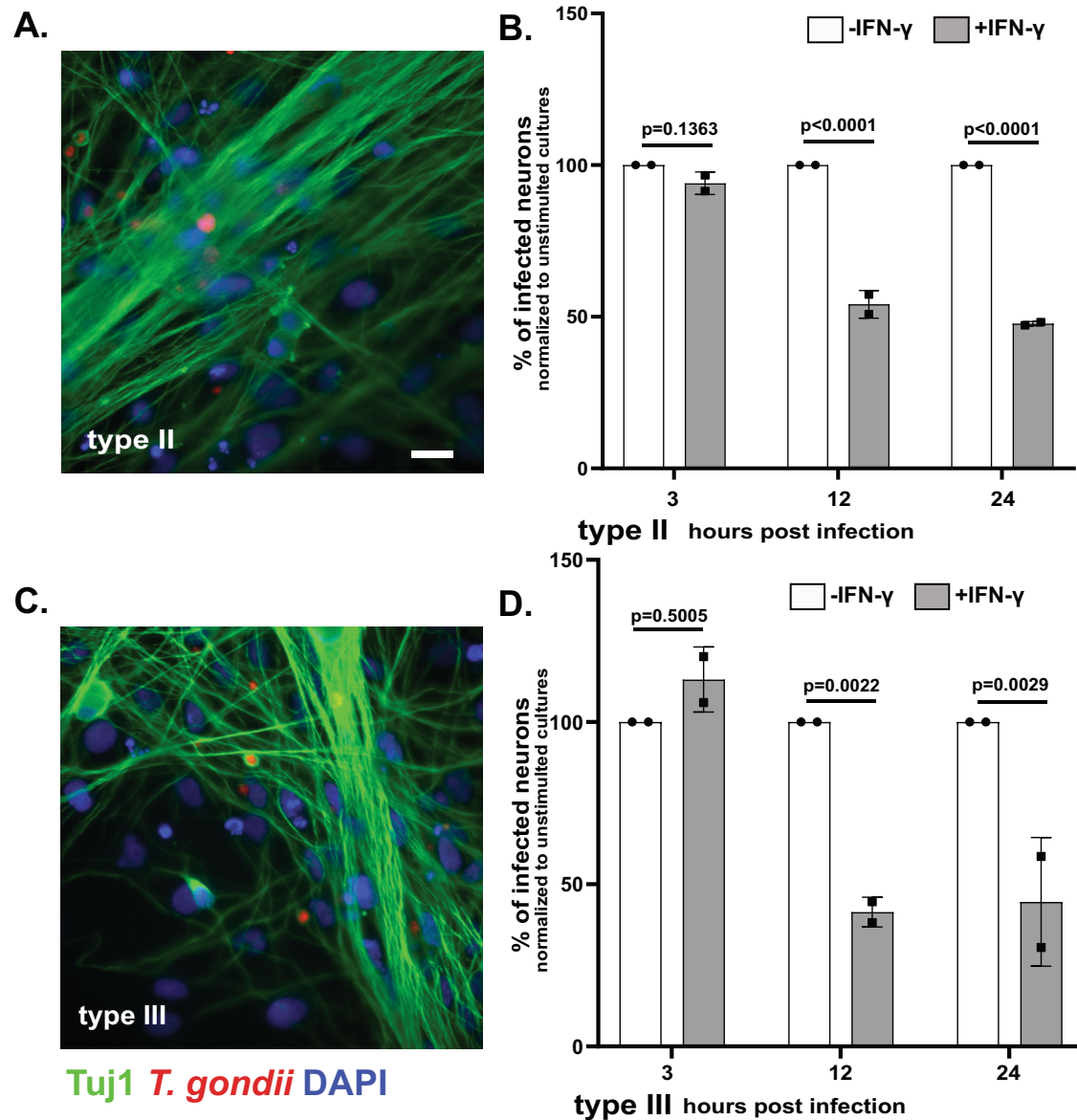


Fig. 6 | IFN- γ stimulation of human neurons leads to a decrease in the percentage infected with *T. gondii*. Human neurons cultures were stimulated with human IFN- γ (100 U/ml) or vehicle for 24 h, followed by infection with listed *T. gondii* strains. At listed time points, cultures were fixed, stained with anti-TuJ1 antibodies and DAPI, and analyzed on an Operetta[®] CLS[™] high content analysis microscope. **A** Representative images of human neurons infected with type II

parasites. Green = anti-TuJ1 antibodies, red = mCherry expressing parasites, blue = DAPI. Scale bar = 20 μ m. **B** Graph of the rate of type II infected neurons at the listed time points, normalized to the unstimulated culture. **C** As in **A** except for type III parasites. **D** As in **B** except for type III parasites. **B, D** Bars mean \pm SD. $N = 1100$ –1450 neurons/*T. gondii* strain/experiment, 2 independent differentiations. 2-way ANOVA with Sidak's multiple comparisons. Source data are provided as a Source Data file.

by neurons affects CNS parasite control²⁶. This work showed that murine CNS cyst burden varied depending on neuron expression of a specific MHC I allele but did not determine if the changes in cyst burden arose from cytolytic clearance of infected neurons; induction of IFN- γ secretion by CD8⁺ T cells; or even non-cytolytic, perforin-dependent clearance of parasites by CD8⁺ T cells⁵⁷. Our data that infected neurons clear intracellular parasites in vivo (Fig. 5E) establish that a non-cytolytic mechanism of clearance occurs and our in vitro work (Figs. 2–4) suggests that IFN- γ -dependent, cell-intrinsic clearance is more likely. Finally, as the Cre reporter mice we use only express the class I MHC H-2 L^b, these data suggest that productive CD8⁺ T cell-neuron interactions also occur in wild type B6 mice.

In human neurons, the data presented here show that IFN- γ stimulation leads to a ~50% reduction in the neuron infection rate, which is consistent with the rate of clearance marker loading on PVs in IFN- γ -stimulated primary human umbilical vein endothelial cells⁵⁸.

Currently, we cannot distinguish between an IFN- γ -dependent invasion defect or clearance of intracellular parasites or both. Though we cannot discriminate between these possibilities, the IFN- γ -dependent, anti-parasite effect appears to have a more robust effect on hPSC neuron infection rates compared to murine neurons (50 vs. 25%). What mechanisms underlie this impressive IFN- γ -dependent resistance to *T. gondii* infection will be the subject of future studies.

Though we have shown that IFN- γ -stimulated neurons can clear parasites in an IRG-dependent manner, our data also suggests that major cell-specific differences in IRG efficiency exist. We found that in vitro, ~20–25% of intracellular parasites will be cleared by neurons in an IFN- γ , IRG-dependent manner, while other groups have shown that IFN- γ stimulated murine astrocytes, macrophages, and fibroblasts have higher rates of Irga6⁺ loading (50–75%) and clearance over a much shorter time (1–2 h post-infection)^{33,59,60}. While some of the difference may be secondary to technical differences (e.g., use of antibody vs.

transfection of Irga6-tagged with GFP, different MOIs), part of the difference is likely secondary to a blunted cell-intrinsic immune response from neurons (as suggested by the undetectable levels of baseline STAT1). Other, not mutually exclusive possibilities include that IRG-clearance differs between neuronal subcellular locations (i.e., it might be expensive to put IRG-machinery along the whole neuron) and/or that full neuron responses require direct interactions with other cell types such as astrocytes or T cells.

Our *in vivo* data using II-GCre parasites are consistent with the possibility that other cell types influence neuronal clearance of intracellular parasites. *In vivo* we found that ~50% of II-GCre-triggered GFP⁺ neurons do not harbor parasites (Fig. 5). This rate of neuronal clearance is approximately double what we observed *in vitro*. In the *in vivo* setting, neurons are in constant communication with other cell types (e.g. astrocytes, microglia, infiltrating T cells), which may potentiate IRG-dependent clearance or initiate complementary methods for clearing intracellular parasites (e.g. CD40-dependent xenophagy^{61,62}). Understanding why neurons incompletely clear parasites and how to improve this clearance is essential for developing curative anti-*T. gondii* therapies. Future studies will focus on mechanistically defining these *in vivo* vs. *in vitro* differences and what inhibits neuron clearance.

In summary, our findings offer substantial evidence that IFN- γ pre-stimulation enables murine and human neurons to mount anti-parasitic defenses against *T. gondii*. While much work is left to be done to understand these anti-parasitic defenses, the work presented here suggests that *T. gondii*'s persistence in neurons is not simply a foregone conclusion.

Methods

Parasite maintenance

The parasite strains used in this study were maintained through serial passage in human foreskin fibroblasts (HFFs) using DMEM, supplemented with 10% fetal bovine serum (FBS), 2 mM Glutagro and 100 IU/ml penicillin and 100 μ g/ml streptomycin. Except for the type II (Prugniaud) strain that expresses Gra16::Cre (II-GCre), the *T. gondii* strains used have been previously described^{15,27}.

Generation of GCre parasites

To generate Gra16::Cre *T. gondii* parasites, we used standard molecular methods²⁷. In brief, we modified a previously described plasmid—that expresses the selectable hypoxanthine xanthine guanine phosphoribosyl transferase (HPT) marker and an epitope tagged rhostry protein fused to an NLS and Cre recombinase (*ptoxoflin-Cre*)²⁸—by inserting the 5' UTR (1000 bp) and coding DNA sequences (CDS) for dense granule protein 16 (pGra16-Cre) in front of the Cre CDS using standard In-Fusion cloning (Takara Bio, 638918). The primers are listed in Supplementary Table 1. The parental type II strain type (Pru Δ hpt) was electroporated with the pGra16-Cre plasmid after linearization upstream of the relevant expression cassettes. The parasites were then subjected to several rounds of selection for HPT expression using medium containing 25 μ g/ml mycophenolic acid and 50 μ g/ml xanthine followed by cloning by limiting dilution⁶³. Single cell clones that were HPT⁺ and confirmed to express the appropriate Gra16 fusion protein were then tested for efficacy in causing Cre-mediated recombination in a Cre-reporter cell line.

Mice

All procedures and experiments were carried out in accordance with the Public Health Service Policy on Human Care and Use of Laboratory Animals and approved by the University of Arizona's Institutional Animal Care and Use Committee (#12-391). All mice were bred and housed in specific-pathogen-free University of Arizona Animal Care facilities with a 14 hr/10 hr light/dark cycle, with ambient temperature

between 68° and 75° F, and 30–70% humidity. Cre reporter mice⁶⁴ (#007906) were originally purchased from Jackson Laboratories. Breeding pairs of *Irgm1/m3*^{-/-} (*Irgm1/3* KO) mice⁵⁰ were generously provided by Greg Taylor (Duke University, Durham, NC).

In vivo infection with GCre parasites

Cre reporter mice were intraperitoneally infected with 10,000 or 20,000 freshly lysed Gra16-Cre (II-GCre) parasites. Brains were harvested at 21 dpi followed by drop fixation in 4% PFA at 4 °C overnight before being transferred and stored in 30% sucrose until they were sectioned. *T. gondii* infected, sucrose embedded brains were sagittally sectioned to 200 μ m on a vibratome and stored in cryoprotectant media (0.05 M sodium phosphate buffer containing 30% glycerol and 30% ethylene glycol). Sections were cleared using a modified PACT clearing protocol previously described⁵³. In brief, sections were incubated overnight in a hydrogel monomer solution at 4 °C and deoxygenated the next morning by bubbling nitrogen gas into sample vials. Samples were incubated at 42 °C to initiate crosslinking of proteins, washed, and incubated in 8% sodium dodecyl sulfate (SDS) at 45 °C to remove lipids. After multiple wash steps to remove SDS from the sections, nuclei were stained using Hoechst. Samples were then washed and submerged overnight in sorbitol refractive index matching solution (sRIMS) consisting of 70% Sorbitol and 0.01% NaN₃ dissolved in 0.02 M PB, followed by mounting on spacer slides in fresh sRIMS. Mounted sections were then imaged at 40 \times magnification using a Zeiss NLO 880 confocal microscope (Imaging Core—Marley, University of Arizona)⁵⁴. We created z-stack tile scans of each neuron to ensure capturing as much of the neuron's axon and processes as were available in each section. Stitched images were converted to Imaris files and imported into Bitplane Imaris software (IMARIS Software X64; Version 9.7.2), where neuronal projections were rendered using the filaments tool.

Primary murine neuron cultures

Primary neurons were cultured by previously described methods with minor modifications⁶⁵. Culture plates were coated overnight with either 0.001% poly-L-lysine (Sigma, Cat # P4707) solution for plastic surfaces or 100 μ g/ml poly-L-lysine hydrobromide (Sigma, Cat # P6282) for glass surfaces. Neurons were seeded in plating media, which is MEM (Thermo Fisher, Cat #11095080) supplemented with 0.6% D-glucose (Sigma, Cat # G8270), L-Glutamine (Thermo Fisher, Cat # 25030024), and 5% fetal bovine serum (FBS) (Thermo Fisher, Cat # 26140079) at appropriate densities: 500,000 in 6-well plates for RNA and protein extraction, 100,000 in 24 well plates with coverslips for imaging, and 20,000 in 96 well plates for counting. Four hours after plating, the media was changed to complete neurobasal media, which consists of Neurobasal™ media (Thermo Fisher, Cat # 21103049) supplemented with B27 (Thermo Fisher, Cat # 17504001), L-Glutamine and Penicillin/Streptomycin (Thermo Fisher, Cat # 15070063) antibiotic cocktail. On day *in vitro* (DIV) 4, neurons received a half volume media change of complete neurobasal media with 5 μ M cytosine arabinoside to stop glial proliferation. Thereafter, one third media exchanges with complete neurobasal media occurred every 3-4 days. All the experiments were performed on 12 DIV neurons.

IFN- γ stimulation and *T. gondii* infection

Primary neurons were pre-stimulated with 100 U/ml of mouse recombinant IFN- γ (R&D Systems, Cat # 485-MI-100) for 4 & 24 h (RNA extraction), 24 & 48 h (protein extraction), or 24 h (*T. gondii* infections). Freshly syringe-lysed *T. gondii* parasites resuspended in complete neurobasal media were used to infect the primary neurons at MOI=4 (for 3 hpi), MOI=2 (For 12 hpi), MOI=1 (for 24 hpi) and MOI=0.2 (for 48 and 72 hpi) time points.

Quantitative real time PCR

For gene expression quantification, RNA was extracted from 4 h and 24 h IFN- γ stimulated primary neurons using TRIzol™ Reagent (Life Technologies) and following the manufacturer's protocol. 500 ng of total RNA was converted into first strand cDNA using a High-Capacity cDNA Reverse Transcription Kit (Applied Biosystems™; Cat No: 4368814) and following the manufacturer's instructions. Using the primers listed in Supplementary Table S1, IFN- γ response and IRG pathway genes were amplified using SYBR green fluorescence detection with an Eppendorf Mastercycler ep realplex 2.2 system. GAPDH was used as a housekeeping gene to normalize RNA levels. Results were calculated using the $2^{-\Delta\Delta CT}$ method⁶⁶.

Protein extraction and Western blotting

Primary neurons were either unstimulated or stimulated with IFN- γ for 24 h and 48 h, followed by total protein extraction as previously described⁶⁷. Equal amounts of protein were subjected to SDS-PAGE, transferred to PVDF membrane and western blotting was done by standard methods. The blots were imaged using the Odyssey Infrared Imaging Systems (LI-COR Biosciences) and quantification was done using Image Studio software (Version 5.2).

Murine neuronal clearance assay

Primary neurons (wild type or Irgm1/3 KO) plated were plated on a poly-L-lysine coated 96-well plate (20,000/well) and were either unstimulated or pre-stimulated with IFN- γ for 24 h prior to infection with mCherry-expressing *T. gondii* parasites. The cells were then fixed and labeled with anti-NeuN antibodies (neuronal nuclei) and DAPI (all nuclei). Wells were imaged using an Operetta™ CLS™ high content analysis system (Functional Genomics Core, University of Arizona). Generated images were then analyzed using Image J software (NIH, Version 1.52 K). All results were normalized to the neuron infection rate in the unstimulated group.

For assays involving II-GCre parasites, neurons from either wild type (Cre reporter) or Cre reporter Irgm1/3 KO mice were plated on poly-L-lysine coated 6 well plates (500,000/well). At the appropriate DIV, the neurons were either stimulated with IFN- γ or vehicle for 24 h followed by infection with II-GCre parasites. At 72 hpi, the plates were processed as described above. Fixed and stained plates were then analyzed using an epifluorescent microscope (EVOS). The person analyzing the images was blinded to IFN- γ stimulation and/or infecting parasite strain.

Immunofluorescence assay

Cells were grown on poly-L-lysine-coated glass coverslips (described above) and were processed by methods as previously described⁶⁵.

Antibodies

The following primary antibodies were used in the study: mouse anti-tubulin beta III isoform (Tuj1), clone TU20 (MAB1637, Millipore, 1:1000); rabbit anti- β 3-Tubulin, D7IG9 (similar to Tuj1) (5568 S, CST, 1:1000); mouse anti-NeuN clone A60 (MAB377, Millipore, 1:1000); rabbit anti-Glial Fibrillary Acidic protein (GFAP) (Z0334, DAKO, 1:500); rabbit anti-S100 (Z0311, DAKO, 1:500); rabbit anti-ALDH1L1 (Ab87117, Abcam, 1:500); chicken anti-Iba1 (Ab 139590, Abcam, 1:500), rabbit anti-STAT1 (Ab47425, Abcam; 1:500); mouse anti-pSTAT1 pY701 clone14/p-STAT1 (612132, BD Biosciences, 1:250); rabbit anti-pSTAT1 Tyr701, Clone 58D6 (9167, CST, 1:200); rabbit anti-*T. gondii* polyclonal antibody (PA-17252, ThermoFisher, 1:5000); mouse anti-SAG1 DG52 (gift John Boothroyd, 1:10,000)⁶⁸; mouse anti-SRS9 (gift John Boothroyd, 1:10,000) (Kim and Boothroyd, 2005); mouse anti-Irga6 (1:1500), mouse anti-Irgb6 (1:250) (gift Jonathan Howard)³³; rabbit anti-HA C29F4 (3724 S, CST, 1:500); mouse anti-ROP2/4 (1:1000, gift John Boothroyd)⁶⁹; mouse anti-SAG2X (1:2000, gift John Boothroyd)⁷⁰; DAPI (D3571, Thermo Fisher, 1:1000); Hoechst 33342 Trihydrochloride,

Trihydrate (H3570, Thermo Fisher, 1:1000). The following species-appropriate secondary antibodies were used: Alexa Fluor 405 goat anti-rabbit IgG, Alexa Fluor 488 goat anti-mouse IgG, Alexa Fluor 568 goat anti-rabbit IgG, Alexa Fluor 647 goat anti-mouse IgG, Alexa Fluor 647 goat anti-chicken IgG, Alexa Fluor 647 goat anti-rabbit IgG, donkey anti-mouse IgG, DyLight 680 conjugate (1:10000), and donkey anti-rabbit IgG, DyLight 800 conjugate (1:10000). Unless otherwise noted, secondary antibodies were obtained from Life Technologies and used at a concentration of 1:500.

Human pluripotent stem cell derived neurons

Human embryonic neural stem cells (NSCs) derived from the NIH-approved H7 embryonic stem cells (WiCell WA07) were purchased from the University of Arizona iPSC core (<https://stemcells.arizona.edu/>). All procedures and experiments were approved by the University of Arizona's Embryonic Stem Cell Research Oversight (ESCRO) Committee. The NSCs were expanded and differentiated into cortical layer neurons using a previously described protocol⁷¹ with minor modifications. Briefly, NSCs were expanded on Matrigel™ Matrix (Corning®, #354277) coated plates using NSC expansion medium (NEM) (ThermoFisher, Cat # A1647801). The media was changed every other day until NSCs reached confluence. For differentiation to cortical neurons, P2 passaged NSCs were plated on poly-L-ornithine (20 μ g/ml) (Sigma, Cat # P4957) and laminin (5 μ g/ml) (Thermo Fisher, Cat # 23017015) coated plates and differentiated for 14 days, using neural differentiation medium (NDM), which consists of Neurobasal™ medium, 2 mM L-Glutamine, 1% B-27, 200 μ M L-Ascorbic acid (Sigma, Cat # A92902), 0.5 mM c-AMP (Stem Cell Technologies Cat # 73886), 20 ng/ml BDNF (Stem Cell Technologies Cat # 78005), 20 ng/ml GDNF (Stem Cell Technologies Cat # 78058), 20 ng/ml NT-3 (Stem Cell Technologies Cat # 78074), and Penicillin/Streptomycin cocktail. The culture medium was exchanged with fresh NDM every 2–3 days.

Human neuronal clearance assay

The clearance assay in human neurons was performed as described for murine neurons except that human IFN- γ (R&D Systems, Cat # 285-MI-100) was used for pre-stimulation.

Statistical analyses

Graphs were generated and statistical analyses were performed using Graphpad Prism 9.1.2 software. The specific test used (e.g., ANOVA vs. *t*-test) is noted in each Figure.

Reporting summary

Further information on research design is available in the Nature Research Reporting Summary linked to this article.

Data availability

Source data for Figs. 1–6 and Supplementary Figs. 1–3 are provided with this paper. Source data are provided with this paper.

References

- Joly, E., Mucke, L. & Oldstone, M. B. A. Viral persistence in neurons explained by lack of major histocompatibility class I expression. *Science* **253**, 1283–1286 (1991).
- Oldstone, M. B., Blount, P., Southern, P. J. & Lampert, P. W. Cytoimmunotherapy for persistent virus infection reveals a unique clearance pattern from the central nervous system. *Nature* **321**, 239–243 (1986).
- Rall, G. F., Mucke, L. & Oldstone, M. B. Consequences of cytotoxic T lymphocyte interaction with major histocompatibility complex class I-expressing neurons in vivo. *J. Exp. Med.* **182**, 1201–1212 (1995).
- Neumann, H., Cavalié, A., Jenne, D. E. & Wekerle, H. Induction of MHC class I genes in neurons. *Science* **269**, 549–552 (1995).

5. Rose, R. W., Vorobyeva, A. G., Skipworth, J. D., Nicolas, E. & Rall, G. F. Altered levels of STAT1 and STAT3 influence the neuronal response to interferon gamma. *J. Neuroimmunol.* **192**, 145–156 (2007).
6. Wong, G. H. W., Bartlett, P. F., Clark-Lewis, I., Batty, F. & Schrader, J. W. Inducible expression of H-2 and Ia antigens on brain cells. *Nature* **310**, 688–691 (1984).
7. Delhay, S. et al. Neurons produce type I interferon during viral encephalitis. *Proc. Natl Acad. Sci. USA* **103**, 7835–7840 (2006).
8. Neumann, H., Schmidt, H., Cavalié, A., Jenne, D. & Wekerle, H. Major histocompatibility complex (MHC) Class I gene expression in single neurons of the central nervous system: differential regulation by interferon (IFN)- γ and tumor necrosis factor (TNF)- α . *J. Exp. Med.* **185**, 305–316 (1997).
9. Binder, G. K. & Griffin, D. E. Interferon- γ -mediated site-specific clearance of alphavirus from CNS neurons. *Science* **293**, 303–306 (2001).
10. Orvedahl, A. et al. Autophagy protects against Sindbis virus infection of the central nervous system. *Cell Host Microbe* **7**, 115–127 (2010).
11. Detje, C. N. et al. Local type I IFN receptor signaling protects against virus spread within the central nervous system. *J. Immunol.* **182**, 2297–2304 (2009).
12. Ferguson, D. J. & Hutchison, W. M. The host-parasite relationship of *Toxoplasma gondii* in the brains of chronically infected mice. *Virchows Arch. A Pathol. Anat. Histopathol.* **411**, 39–43 (1987).
13. Ferguson, D. J. P. & Hutchison, W. M. An ultrastructural study of the early development and tissue cyst formation of *Toxoplasma gondii* in the brains of mice. *Parasitol. Res.* **73**, 483–491 (1987).
14. Melzer, T. C., Cranston, H. J., Weiss, L. M. & Halonen, S. K. Host cell preference of *Toxoplasma gondii* cysts in murine brain: a confocal study. *J. Neuroparasitology.* **1**, 1–6 (2010).
15. Cabral, C. M. et al. Neurons are the primary target cell for the brain-tropic intracellular parasite *Toxoplasma gondii*. *PLoS Pathog.* **12**, e1005447 (2016).
16. Suzuki, Y., Conley, F. K. & Remington, J. S. Importance of endogenous IFN- γ for prevention of toxoplasmic encephalitis in mice. *J. Immunol.* **143**, 2045–2050 (1989).
17. Suzuki, Y., Orellana, M. A., Schreiber, R. D. & Remington, J. S. Interferon- γ : the major mediator of resistance against *Toxoplasma gondii*. *Science* **240**, 516–518 (1988).
18. Collazo, C. M. et al. The function of gamma interferon-inducible GTP-binding protein IGTP in host resistance to *Toxoplasma gondii* is Stat1 dependent and requires expression in both hematopoietic and nonhematopoietic cellular compartments. *Infect. Immun.* **70**, 6933–6939 (2002).
19. Halonen, S. K., Taylor, G. A. & Weiss, L. M. Gamma interferon-induced inhibition of *Toxoplasma gondii* in astrocytes is mediated by IGTP. *Infect. Immun.* **69**, 5573–5576 (2001).
20. Taylor, G. A. et al. Pathogen-specific loss of host resistance in mice lacking the IFN- γ -inducible gene IGTP. *Proc. Natl Acad. Sci. USA* **97**, 751–755 (2000).
21. Halonen, S. K., Chiu, F. & Weiss, L. M. Effect of cytokines on growth of *Toxoplasma gondii* in murine astrocytes. *Infect. Immun.* **66**, 4989–4993 (1998).
22. Jones, T. C., Bienz, K. A. & Erb, P. In vitro cultivation of *Toxoplasma gondii* cysts in astrocytes in the presence of gamma interferon. *Infect. Immun.* **51**, 147–156 (1986).
23. Schluter, D., Deckert, M., Hof, H. & Frei, K. *Toxoplasma gondii* infection of neurons induces neuronal cytokine and chemokine production, but gamma interferon- and tumor necrosis factor-stimulated neurons fail to inhibit the invasion and growth of *T. gondii*. *Infect. Immun.* **69**, 7889–7893 (2001).
24. Brown, C. R. et al. Definitive identification of a gene that confers resistance against *Toxoplasma* cyst burden and encephalitis. *Immunology* **85**, 419–428 (1995).
25. Blanchard, N. et al. Immunodominant, protective response to the parasite *Toxoplasma gondii* requires antigen processing in the endoplasmic reticulum. *Nat. Immunol.* **9**, 937–944 (2008).
26. Salvioni, A. et al. Robust control of a brain-persisting parasite through MHC I presentation by infected neurons. *Cell Rep.* **27**, 3254–3268.e8 (2019).
27. Koshy, A. A. et al. *Toxoplasma* co-opts host cells it does not invade. *PLoS Pathog.* **8**, e1002825 (2012).
28. Koshy, A. A. et al. *Toxoplasma* secreting Cre recombinase for analysis of host-parasite interactions. *Nat. Methods* **7**, 307–309 (2010).
29. Berenreiterová, M., Flegr, J., Kuběna, A. A. & Nĕmec, P. The distribution of *Toxoplasma gondii* cysts in the brain of a mouse with latent toxoplasmosis: implications for the behavioral manipulation hypothesis. *PLoS ONE* **6**, e28925 (2011).
30. Mendez, O. A. et al. Semi-automated quantification and neuroanatomical mapping of heterogeneous cell populations. *J. Neurosci. Methods* **305**, 98–104 (2018).
31. Boillat, M. et al. Neuroinflammation-associated aspecific manipulation of mouse predator fear by *Toxoplasma gondii*. *Cell Rep.* **30**, 320–334.e6 (2020).
32. Howard, J. C., Hunn, J. P. & Steinfeldt, T. The IRG protein-based resistance mechanism in mice and its relation to virulence in *Toxoplasma gondii*. *Curr. Opin. Microbiol.* **14**, 414–421 (2011).
33. Khaminets, A. et al. Coordinated loading of IRG resistance GTPases on to the *Toxoplasma gondii* parasitophorous vacuole. *Cell. Microbiol.* **12**, 939–961 (2010).
34. Degrandi, D. et al. Murine Guanylate Binding Protein 2 (mGBP2) controls *Toxoplasma gondii* replication. *Proc. Natl Acad. Sci. USA* **110**, 294–299 (2013).
35. Lafuse, W. P., Brown, D., Castle, L. & Zwilling, B. S. Cloning and characterization of a novel cDNA that is IFN- γ -induced in mouse peritoneal macrophages and encodes a putative GTP-binding protein. *J. Leukoc. Biol.* **57**, 477–483 (1995).
36. Boehm, U. et al. Two families of GTPases dominate the complex cellular response to IFN- γ . *J. Immunol.* **161**, 6715–6723 (1998).
37. O'Donnell, L. A. et al. Interferon gamma induces protective non-canonical signaling pathways in primary neurons. *J. Neurochem.* **135**, 309–322 (2015).
38. Howe, D. K. & Sibley, L. D. *Toxoplasma gondii* comprises three clonal lineages: correlation of parasite genotype with human disease. *J. Infect. Dis.* **172**, 1561–1566 (1995).
39. Sibley, L. D. & Boothroyd, J. C. Virulent strains of *Toxoplasma gondii* comprise a single clonal lineage. *Nature* **359**, 82–85 (1992).
40. Braun, L. et al. A *Toxoplasma* dense granule protein, GRA24, modulates the early immune response to infection by promoting a direct and sustained host p38 MAPK activation. *J. Exp. Med.* **210**, 2071–2086 (2013).
41. Franco, M. et al. A novel secreted protein, MYR1, is central to *Toxoplasma*'s manipulation of host cells. *mBio* **7**, e02231–02215 (2016).
42. Gay, G. et al. *Toxoplasma gondii* TgIST co-opts host chromatin repressors dampening STAT1-dependent gene regulation and IFN- γ -mediated host defenses. *J. Exp. Med.* **213**, 1779–1798 (2016).
43. Bougdour, A. et al. Host cell subversion by *Toxoplasma* GRA16, an exported dense granule protein that targets the host cell nucleus and alters gene expression. *Cell Host Microbe* **13**, 489–500 (2013).
44. Curt-Varesano, A., Braun, L., Ranquet, C., Hakimi, M.-A. & Bougdour, A. The aspartyl protease TgASP5 mediates the export of the *Toxoplasma* GRA16 and GRA24 effectors into host cells. *Cell. Microbiol.* **18**, 151–167 (2016).

45. Bracha, S. et al. Engineering Brain Parasites for Intracellular Delivery of Therapeutic Proteins. *bioRxiv* 481192 <https://doi.org/10.1101/481192> (2018).
46. Zhao, Y. O., Khaminets, A., Hunn, J. P. & Howard, J. C. Disruption of the *Toxoplasma gondii* parasitophorous vacuole by IFN γ -inducible immunity-related GTPases (IRG proteins) triggers necrotic cell death. *PLoS Pathog.* **5**, e1000288 (2009).
47. Hermanns, T., Müller, U. B., Könen-Waisman, S., Howard, J. C. & Steinfeldt, T. The *Toxoplasma gondii* rhopty protein ROP18 is an Irga6-specific kinase and regulated by the dense granule protein GRA7. *Cell. Microbiol.* **18**, 244–259 (2016).
48. Saeij, J. P. J. et al. Polymorphic secreted kinases are key virulence factors in toxoplasmosis. *Science* **314**, 1780–1783 (2006).
49. Taylor, S. et al. A secreted serine-threonine kinase determines virulence in the eukaryotic pathogen *Toxoplasma gondii*. *Science* **314**, 1776–1780 (2006).
50. Collazo, C. M. et al. Inactivation of *Lrg-47* and *Irg-47* reveals a family of interferon γ -inducible genes with essential, pathogen-specific roles in resistance to infection. *J. Exp. Med.* **194**, 181–188 (2001).
51. Hunn, J. P. et al. Regulatory interactions between IRG resistance GTPases in the cellular response to *Toxoplasma gondii*. *EMBO J.* **27**, 2495–2509 (2008).
52. Henry, S. C. et al. Balance of *Irgm* protein activities determines IFN- γ -induced host defense. *J. Leukoc. Biol.* **85**, 877–885 (2009).
53. Cabral, C. M., Merritt, E. F. & Koshy, A. A. Three-dimensional reconstruction of toxoplasma-neuron interactions in situ. *Methods Mol. Biol.* **2071**, 283–295 (2020).
54. Koshy, A. A. & Cabral, C. M. 3-D imaging and analysis of neurons infected in vivo with *Toxoplasma gondii*. *J. Vis. Exp.* <https://doi.org/10.3791/52237> (2014).
55. Fisch, D., Clough, B. & Frickel, E.-M. Human immunity to *Toxoplasma gondii*. *PLOS Pathog.* **15**, e1008097 (2019).
56. Bando, H. et al. *Toxoplasma* effector GRA15-dependent suppression of IFN- γ -induced antiparasitic response in human neurons. *Front. Cell. Infect. Microbiol.* **9**, 140 (2019).
57. Suzuki, Y. et al. Removal of *Toxoplasma gondii* cysts from the brain by perforin-mediated activity of CD8+ T cells. *Am. J. Pathol.* **176**, 1607–1613 (2010).
58. Clough, B. et al. K63-linked ubiquitination targets *Toxoplasma gondii* for endo-lysosomal destruction in IFN γ -stimulated human cells. *PLOS Pathog.* **12**, e1006027 (2016).
59. MacMicking, J. D. Interferon-inducible effector mechanisms in cell-autonomous immunity. *Nat. Rev. Immunol.* **12**, 367–382 (2012).
60. Martens, S. et al. Disruption of *Toxoplasma gondii* parasitophorous vacuoles by the mouse p47-resistance GTPases. *PLOS Pathog.* **1**, e24 (2005).
61. Andrade, R. M., Wessendarp, M., Gubbels, M.-J., Striepen, B. & Subauste, C. S. CD40 induces macrophage anti-*Toxoplasma gondii* activity by triggering autophagy-dependent fusion of pathogen-containing vacuoles and lysosomes. *J. Clin. Invest* **116**, 2366–2377 (2006).
62. Subauste, C. S. CD40, autophagy and *Toxoplasma gondii*. *Mem. Inst. Oswaldo Cruz* **104**, 267–272 (2009).
63. Donald, R. G. K., Carter, D., Ullman, B. & Roos, D. S. Insertional tagging, cloning, and expression of the *Toxoplasma gondii* hypoxanthine-xanthine-guanine phosphoribosyltransferase gene: use as a selectable marker for stable transformation. *J. Biol. Chem.* **271**, 14010–14019 (1996).
64. Madisen, L. et al. A robust and high-throughput Cre reporting and characterization system for the whole mouse brain. *Nat. Neurosci.* **13**, 133–140 (2010).
65. Parker, S. S. et al. High fidelity cryopreservation and recovery of primary rodent cortical neurons. *eNeuro* **5**, ENEURO.0135-18.2018 (2018).
66. Livak, K. J. & Schmittgen, T. D. Analysis of relative gene expression data using real-time quantitative PCR and the 2- $\Delta\Delta$ CT method. *Methods* **25**, 402–408 (2001).
67. Cabral, C. M., McGovern, K. E., MacDonald, W. R., Franco, J. & Koshy, A. A. Dissecting amyloid beta deposition using distinct strains of the neurotropic parasite *Toxoplasma gondii* as a novel tool. *ASN Neuro* **9**, 1759091417724915 (2017).
68. Burg, J. L., Perelman, D., Kasper, L. H., Ware, P. L. & Boothroyd, J. C. Molecular analysis of the gene encoding the major surface antigen of *Toxoplasma gondii*. *J. Immunol.* **141**, 3584–3591 (1988).
69. Sadak, A., Taghy, Z., Fortier, B. & Dubremetz, J. F. Characterization of a family of rhopty proteins of *Toxoplasma gondii*. *Mol. Biochem Parasitol.* **29**, 203–211 (1988).
70. Saeij, J. P. J., Boyle, J. P., Grigg, M. E., Arrizabalaga, G. & Boothroyd, J. C. Bioluminescence imaging of *Toxoplasma gondii* infection in living mice reveals dramatic differences between strains. *Infect. Immun.* **73**, 695–702 (2005).
71. Yan, Y. et al. Efficient and rapid derivation of primitive neural stem cells and generation of brain subtype neurons from human pluripotent stem cells. *Stem Cells Transl. Med.* **2**, 862–870 (2013).

Acknowledgements

We would like to thank all members of the Koshy Lab for helpful discussions, and especially Kaitlin Thomas for her critical review of the manuscript. We would like thank Greg Taylor (Duke University), for providing us with breeding pairs for *Irgm1/3* KO mice and Jonathan Howard (Instituto Gulbenkian de Ciência), for providing us with anti-Irga6 antibodies. We offer many thanks to Dr. Jared Churko (University of Arizona) and Dr. Rita Sattler (Barrow Neurological Institute) and their lab members for their support with human neuron differentiations. We also thank Dr. Chris Hunter for his careful reading and editing of this manuscript. Funding was provided by the National Institutes of Health (NS095994 (A.A.K.); AI157247 (AAK co-PI); AI147711 (J.A.K.)) and the BIO5 Institute, University of Arizona (A.A.K., S.C.). The funders had no role in study design, data collection and analysis, decision to publish, or preparation of the manuscript.

Author contributions

S.C., J.A.K., E.F.M. designed and performed experiments, validated methodologies, curated data, and analyzed data. S.C. wrote the original draft of the paper with J.A.K. and E.F.M. contributing specific, relevant sections. AAK supervised the project and edited the paper.

Competing interests

The authors have declared that no competing interests exist.

Additional information

Supplementary information The online version contains supplementary material available at <https://doi.org/10.1038/s41467-022-32225-z>.

Correspondence and requests for materials should be addressed to Anita A. Koshy.

Peer review information *Nature Communications* thanks Ildiko Dunay and the other, anonymous, reviewer(s) for their contribution to the peer review of this work. Peer reviewer reports are available.

Reprints and permission information is available at <http://www.nature.com/reprints>

Publisher's note Springer Nature remains neutral with regard to jurisdictional claims in published maps and institutional affiliations.

Open Access This article is licensed under a Creative Commons Attribution 4.0 International License, which permits use, sharing, adaptation, distribution and reproduction in any medium or format, as long as you give appropriate credit to the original author(s) and the source, provide a link to the Creative Commons license, and indicate if changes were made. The images or other third party material in this article are included in the article's Creative Commons license, unless indicated otherwise in a credit line to the material. If material is not included in the article's Creative Commons license and your intended use is not permitted by statutory regulation or exceeds the permitted use, you will need to obtain permission directly from the copyright holder. To view a copy of this license, visit <http://creativecommons.org/licenses/by/4.0/>.

© The Author(s) 2022